Fifth International Conference on CFD in the Process Industries
CSIRO, Melbourne, Australia
13-15 December 2006

UNSTEADY STATE SIMULATION OF EULERIAN-EULERIAN MULTIPHASE FLOW IN FCC RISER REACTORS

N. NOVIA, M. S. RAY, and V. K. PAREEK

Chemical Engineering Department, Curtin University of Technology
GPO Box U1987, Perth 6845, Western Australia

ABSTRACT

Fluid catalytic cracking is the refinery unit operation to convert high-molecular-weight hydrocarbons to higher value products such as gasoline. Optimization of the FCC process is particularly important due to complex interactions between a large number of dependent and independent parameters. The description of multiphase mixing in the riser reactors is an important aspect in an FCC unit. Good solid-fluid mixing is crucial in order to guarantee complete feed vaporization which is important for several reasons, including efficient catalyst-to-oil contact and minimizing coke deposition.

A commercial CFD code Fluent 6.2 was used to simulate the three-dimensional, transient multiphase flow model in FCC riser reactors under different operating conditions. The conservation equations of mass, and momentum for each phase were solved using the Eulerian-Eulerian approach. The simulation results showed good prediction of the flow pattern, velocity profiles and solid volume fraction distribution in the riser.

NOMENCLATURE

C_D	Drag coefficient, [-]
C_μ	Turbulence constant, [-]
d_s	Diameter of solid particles, [m]
e_s	Particle collisions coefficient, [-]
g	Gravitational acceleration, [m s^{-2}]
g_o	Radial distribution function, [-]
$k_{\Theta s}$	Diffusion coefficient, [kg m^{-1} s^{-1}]
k_i	Turbulent kinetic energy, [J kg^{-1}]
P	Static Pressure, [N m^{-1}]
P_s	Solid Pressure, [N m^{-1}]
Re_s	Relative Reynolds number, [-]
T_s	Solid stress tensor, [Pa]
$\mathbf{U}_i$	Velocity of ith phase, [m s^{-1}]
α	Turbulent kinetic energy dissipation rate, [m^2 s^{-3}]
β	Solid gas exchange coefficient, [kg m^{-3} s^{-1}]
ρ_i	Density of ith phase, [kg m^{-3}]
ε_i	Volume fraction of ith phase, [-]
$\in_i$	Turbulent dissipation rate, [m^2 s^{-3}]
τ_i	Shear stress tensor of ith phase, [N m^{-2}]
γ_s	Collisional dissipation of energy, [kg m^{-1} s^{-3}]
Θ_s	Granular temperature, [m^2 s^{-1}]
μ_b	Solid bulk viscosity, [kg m^{-1} s^{-1}]
μ_i	Viscosity of ith phase, [kg m^{-1} s^{-1}]
$\mu_{s,dil}$	Solid phase dilute viscosity, [kg m^{-1} s^{-1}]
μ_t	Turbulent viscosity, [kg m^{-1} s^{-1}]

INTRODUCTION

Complex hydrodynamics of FCC riser reactors is related to the two-phase character of the flow. A model can be a very useful tool for better design and optimal operation, and to predict the flow pattern in the riser as a function of reactor geometry, operating conditions and characteristic of feed and catalyst. Most models reported in the literatures are based on a two-phase description, which consider the catalyst as a particulate phase and the vapour hydrocarbon as a gas phase. The particles are assumed to have identical diameter, density and restitution coefficient.

The aim of this study was to illustrate the Eulerian-Eulerian multiphase flow model to design of FCC riser reactors and to predict the hydrodynamics effect on the operation of the riser. The model predicted the flow pattern of solid; velocity vector of solid phases; and solid volume fraction.

EULERIAN-EULERIAN MULTIPHASE MODEL

Conservation Equations

Continuity equation of phase i (i = gas, solid):

$$\frac{\partial}{\partial t}\left(\rho_i \varepsilon_i\right) + \nabla.\left(\rho_i \varepsilon_i \mathbf{U}_i\right) = 0 \tag{1}$$

Momentum conservation of phase i (i = gas, solid, $k \neq i$):

$$\frac{\partial}{\partial t}\left(\rho_i \varepsilon_i \mathbf{U}_i\right) + \nabla.\left(\rho_i \varepsilon_i \mathbf{U}_i \mathbf{U}_i\right) = -\varepsilon_i \nabla P + \nabla.\tau_i + \rho_i \varepsilon_i g - \beta(U_i - U_k) \tag{2}$$

Interphase Exchange Equations

Syamlal-O'Brien model for the drag force formulation (Fluent, 2005):

$$\beta = \frac{3}{4} C_D \frac{\varepsilon_s \varepsilon_g}{v_{r,s}^2} \frac{\rho_g}{d_s} \left[\frac{\mathrm{Re}_s}{v_{r,s}}\right] \left|U_s - U_g\right| \tag{3}$$

Drag coefficient, C_D is given by:

$$C_D = \left[0.63 + \frac{4.8}{\sqrt{\mathrm{Re}_s}/v_{r,s}}\right]^2 \tag{4}$$

$$\mathrm{Re}_s = \frac{\rho_g d_s \left|U_s - U_g\right|}{\mu_g} \tag{5}$$

Pressure of Solids

Solids phase pressure (P_s) consists of a kinetic term and particle collisions term:

$$Ps = \left(1 + 2\left(1 + e_s\right)\varepsilon_s g_0\right)\varepsilon_s \rho_s \Theta_s = \rho_s \varepsilon_s \Theta_s + 2 g_0 \rho_s \varepsilon_s{}^2 \Theta_s \left(1 + e_s\right) \quad (6)$$

The radial distribution function, g_0 is :

$$g_0 = \left[1 - \left[\frac{\varepsilon_s}{\varepsilon_{s,\max}}\right]^{1/3}\right]^{-1} \quad (7)$$

Solid Shear Stress

Solid phase bulk viscosity:

$$\mu_b = \frac{4}{3}\varepsilon_s \rho_s d_s g_0 \left(1 + e_s\right)\left(\frac{\Theta_s}{\pi}\right)^{1/2} \quad (8)$$

Solid phase shear viscosity:

$$\mu_s = \frac{2\mu_{s,dill}}{\left(1+e\right)g_0}\left[1 + \frac{4}{5}\left(1 + e_s\right)g_0 \varepsilon_s\right]^2 + \frac{4}{5}\varepsilon_s \rho_s d_s g_0 \left(1 + e_s\right)\left[\frac{\Theta_s}{\pi}\right]^{1/2} \quad (9)$$

Solid phase dilute viscosity:

$$\mu_{s,dil} = \frac{5}{16}\rho_s \varepsilon_s l_s \sqrt{2\pi\Theta_s} \quad (10)$$

$$l_s = \frac{\sqrt{2}}{12}\frac{d_s}{\varepsilon_s} \quad (11)$$

Granular Temperature

$$\frac{3}{2}\frac{\partial}{\partial t}\left(\rho_s \varepsilon_s \Theta_s\right) + \nabla.\left(\rho_s \varepsilon_s U_s \Theta_s\right) = T_s : \nabla U_s + \nabla.\left(k_{\Theta s}\nabla\Theta_s\right) - \gamma_s \quad (12)$$

Difusion coefficient for granular energy, $k_{\Theta s}$:

$$k_{\Theta s} = \frac{2k_{\Theta s,dil}}{\left(1+e_s\right)g_0}\left[1 + \frac{6}{5}\left(1 + e_s\right)g_0 \varepsilon_s\right]^2 + 2\varepsilon_s^2 \rho_s d_s g_0 \left(1 + e_s\right)\left[\frac{\Theta_s}{\pi}\right]^{1/2} \quad (13)$$

Where:

$$k_{\Theta s,dil} = \frac{75}{64}\rho_s \varepsilon_s l_s \sqrt{2\pi\Theta_s} \quad (14)$$

Collisional energy dissipation, γ_s, is given by:

$$\gamma_s = 3\left(1 - e_s{}^2\right)\varepsilon_s{}^2 \rho_s g_0 \Theta_s \left[\frac{4}{ds}\left[\frac{\Theta_s}{\pi}\right]^{1/2} - \nabla \mathbf{U}_s\right] \quad (15)$$

k-ε Turbulence Model

The turbulent viscosity is defined as:

$$\mu_{t,i}{}^{(t)} = \rho_i \varepsilon_i C_\mu \frac{k_i{}^2}{\in_i} \quad (16)$$

Turbulent kinetic energy, k, and its rate of dissipation ϵ_i are given by the following transport equations:

$$\frac{\partial}{\partial t}\left(\rho_i \varepsilon_i k_i\right) + \nabla.\left(\rho_i \varepsilon_i k_i U_i\right) = \nabla.\left(\varepsilon_i \frac{\mu_i}{\sigma_k}\nabla k_i\right) + \left(\varepsilon_i G_k - \varepsilon_i \rho_i \in_i\right) \quad (17)$$

$$\frac{\partial}{\partial t}\left(\rho_i \varepsilon_i \in_i\right) + \nabla.\left(\rho_i \varepsilon_i \in_i U_i\right) = \nabla.\left(\varepsilon_i \frac{\mu_i}{\sigma_k}\nabla \in_i\right) + \frac{\in_i}{k}\left(C_{1\in}\varepsilon_i G_k - C_{2\in}\varepsilon_i \rho_i \in_i\right) \quad (18)$$

BOUNDARY CONDITIONS OF FCC RISER REACTORS

In order to produce acceptable simulation results and convergence, appropriate boundary conditions are very important. Initially the riser was empty. At the inlet, all velocities and volume fractions of both phases were specified. At the wall, the gas velocities were set at zero (non-slip condition). It was assumed that instantaneous vaporization of feed as it enters the riser.

The geometries of the FCC riser section are shown in Figure 1. The solid catalyst (zeolite) was injected from the bottom of the riser. Gas-oil feed was fed to the reactor through four nozzles. The angle between the axes of the riser and nozzles was 30°. The riser had a diameter between 1 m at the bottom to 1.4 m at the top. The total of the riser height section simulated was 13.8 m. In order to minimize computational effort, the geometries of the FCC riser section were split into a quarter section of the unit with 5631 computational grids.

The solid catalyst entered the riser at 1 m diameter with flow rate of 200 kg/s. The volume fraction of catalyst was 40%. The average diameter of catalyst particle varied between 10, 60 and 100 μm, and density of about 1500 kg/m^3. The inlet gas-oil velocities were 5, 10 and 15 m/s.

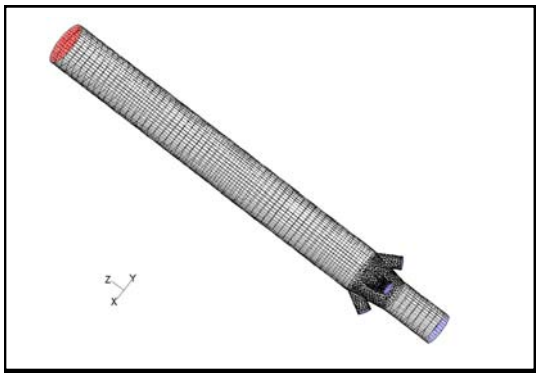

Figure 1: FCC riser reactors geometry (red: outflow; blue: velocity inlet; black: wall).

RESULTS & DISCUSSION

The simulations were carried out to observe the effect of different operating conditions and to describe multiphase flow pattern in the FCC riser reactors. Before using the model, the simulations were carried out using different number of computational cells to understand multiphase behaviour in the riser.

Velocity Vector of Catalyst Particle

It can be seen from Figure 2 that the catalyst is moving upward closely plug flow. The model was not successful in demonstrating the significant down flow near the riser wall. This is because of the model is not neglecting the gas-phase turbulence (Ranade, 1999). The flow pattern in the bottom region of the riser is affected by the geometry of the gas oil feed nozzle and leads to inhomogeneous flow. However, in the upper region, the flow becomes more uniform along the riser height.

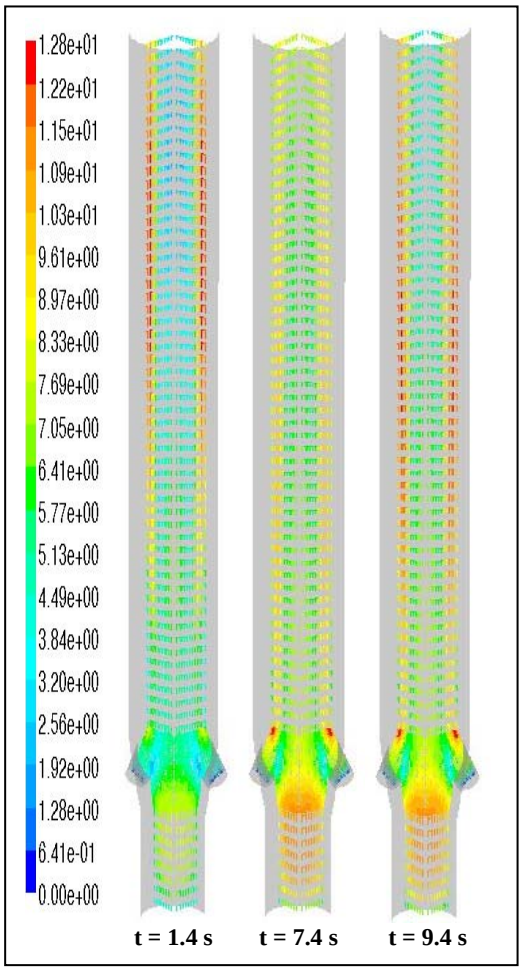

Figure 2: Instantaneous distribution of the velocity vector of catalyst for various simulation times (t = 1.4 s; t = 7.4 s; t = 9.4 s).

In Figure 3, it is found that the velocity profiles of catalyst show an off-centre maximum due to bypassing of the catalyst particles by gas. For this axial direction, the maximum catalyst velocity is observed between the centre and the wall. De Wilde et al. (2005) observed similar flow pattern in their experimental result. They stated that the particles can not follow the gas motion from the central tube to the outer ring of the reactor due to inertia and the gas flow in the outer ring. As shown, the upward velocity of catalyst was quite high at the feed injection nozzles due to low acceleration occurring at the area between the nozzles.

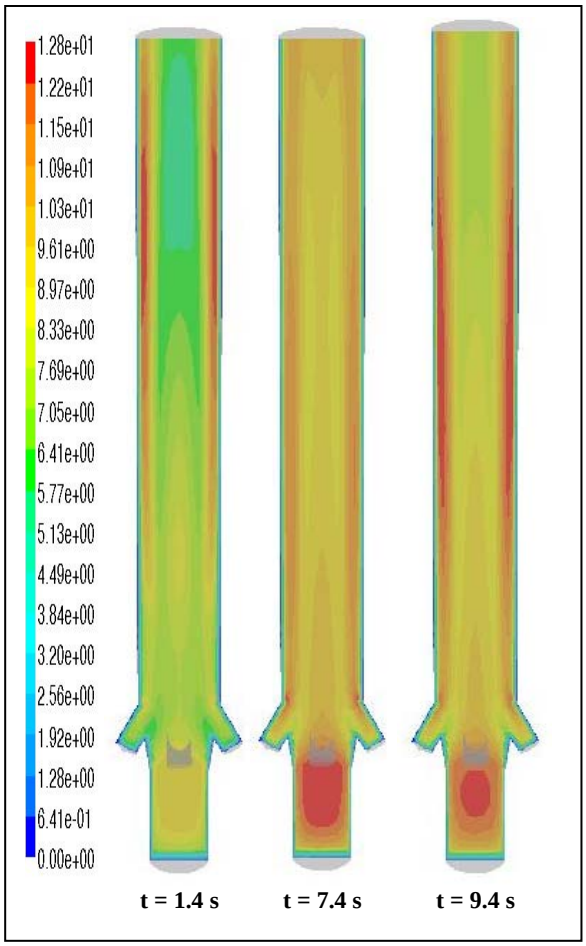

Figure 3 Instantaneous distribution of the velocity magnitude of catalyst for different time (t = 1.4 s; t = 7.4 s; t = 9.4 s).

Contours of Catalyst Volume Fractions

Figure 4 illustrates the time-dependent behaviour of the catalyst volume fraction in the axial cross section of the riser. Contour plots refer to four different times (0.2 s; 0.6 s; 2.6 s; and 3.6 s) from commencing the simulation. Because the catalyst particles enter from the bottom and move toward the top, the increase of solid volume fraction grows from the bottom toward the top of the riser. The typical of radial mixing of particles, as presented in figure 4, show similarities with the previous study by De Wilde et al. (2005). They concluded that radial mixing is better in the bottom zone of the riser.

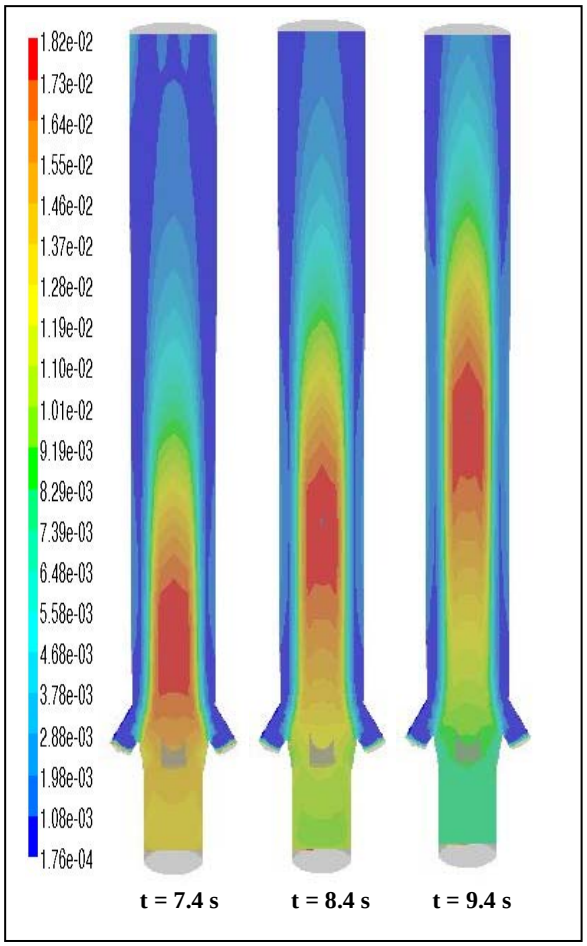

Figure 4: Instantaneous catalyst volume fraction for different time (t = 7.4 s; t = 8.4 s; t = 9.4 s).

Effect of Inlet Gas-Oil Velocity

Figure 5 shows the distribution of the volume fraction of the catalyst obtained for cases with gas-oil velocities of 5, 10, and 15 m/s, solid mass flow rate of 200 kg/s, and diameter of catalyst 60 µm. As shown in Figure 4, the volume fraction of the catalyst decreases across the riser diameter when the gas velocity is increased. Catalyst volume fraction increases regularly from the centre to the wall. These profiles are reasonable agreement with experimental and computed results of Nieuwland et al. (1996)

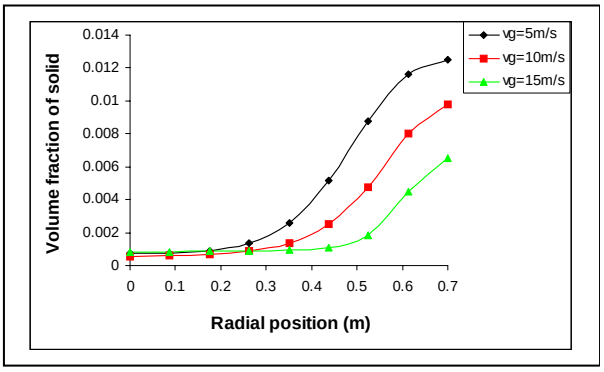

Figure 5: Time-averaged radial catalyst volume fraction at various gas oil velocities.

Effect of Catalyst Size

Figure 6 shows the profiles of the catalyst volume fraction for various catalyst sizes of 10, 60 and 100 µm. The catalyst volume fraction increases with increasing values of the catalyst size. Hence, the model is able to describe quantitatively the accumulation of catalyst at the wall for all different catalyst sizes. Nieuwland (1994) also reported the same profiles especially for solids mass flux of 100 kg m^2 s^{-1} and particle diameter of 129 µm. They used the optical probe system to measure the solid concentration.

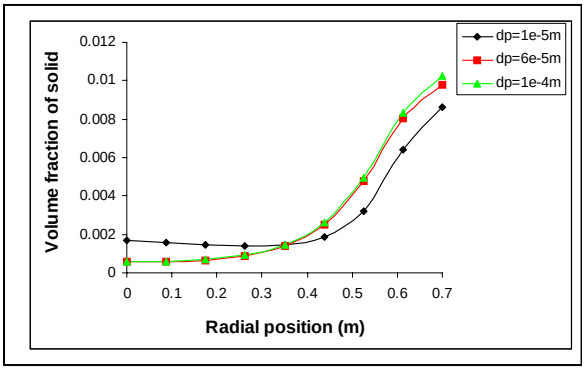

Figure 6: Time-averaged catalyst volume fractions at various catalyst sizes.

CONCLUSIONS

The model shows that the catalyst is moving upward closely plug flow. However, it was not successful in demonstrating the significant down flow near the riser wall. The flow pattern in the bottom region of the riser is affected by the geometry of the gas oil feed nozzle and leads to inhomogeneous flow. The velocity profiles of catalyst show an off-centre maximum due to bypassing of the catalyst particles by gas.

The volume fraction of the solid phase decreases across the riser diameter when the gas velocity is increased. The model is able to describe quantitatively the accumulation of catalyst at the wall for all different catalyst sizes.

REFERENCES

De Wilde, J., Van Engelandt, G., Heynderickx, G. J. and Marin, G. B. (2005), *Gas-solids mixing in the inlet zone of a dilute circulating fluidized bed*, Powder Technol., 151, 96-116.

Fluent (2005), *Fluent 6.2 User Guide*, Lebanon.

Nieuwland, J. J., Huizenga, P., Kuipers, J. A. M. and van Swaaij, W. P. M. (1994), *Hydrodynamic modelling of circulating fluidised beds*, Chem. Eng. Sci., 49, 5803-5811.

Nieuwland, J. J., Meijer, R., Kuipers, J. A. M. and van Swaaij, W. P. M. (1996), Measurements of solids concentration and axial solids velocity in gas-solid two-phase flow, Powder Technol., 87, 127-139.

Ranade, V. V. (1999), Modelling of gas-solid flows in FCC riser reactors: flully developed flow, Second International Conference on CFD in Minerals and Process Industries, 77-82.